

HU-TFT-96-33
September 22, 2018

Continuum extrapolation of energies of a four-quark system in lattice gauge theory

Petrus Pennanen¹

*Research Institute for Theoretical Physics
P.O. Box 9
FIN-00014 University of Helsinki
Finland*

Abstract

A continuum extrapolation of static two- and four-quark energies calculated in quenched SU(2) lattice Monte Carlo is carried out based on Sommer's method of setting the scale. The β -function is obtained as a side product of the extrapolations. Four-quark binding energies are found to be essentially constant at $\beta \geq 2.35$ unlike the two-body potentials. A model for four-quark energies, with explicit gluonic degrees of freedom removed, is fitted to these energies and the behaviour of the parameters of the model is investigated. An extension of the model using the first excited states of the two-body gluon field as additional basis states is found to be necessary for quarks at the corners of regular tetrahedra.

PACS numbers: 11.15.Ha, 12.38.Gc, 13.75.-n, 24.85.+p

¹E-mail: Petrus.Pennanen@helsinki.fi

1 Introduction

Systems of many hadrons play a crucial role in nature and it is important to understand the hadronic interactions from first principles. This would shed light on multi-quark bound states and e.g. meson-meson scattering. A convenient tool for analysing the problem would be a potential model for multi-quark systems with explicit gluonic degrees of freedom removed. Such a model might be based on an effective two-body interaction as in the case of valence electrons in metals and nucleons in nuclei.

Perturbation theory of QCD cannot even treat the confinement of quarks and gluons into hadrons, and the only known way to make realistic calculations of interacting quark clusters are Monte Carlo lattice techniques. Green and coworkers have been simulating systems of four static quarks in quenched SU(2) mainly on $16^3 \times 32$ lattices [1, references therein]. Four quarks, because it is the smallest number that can be partitioned into different colour-singlet groups. Energies of several configurations such as rectangular (R), linear (L) and tetrahedral (T) – examples of which are shown in figure 1 – have been simulated to get a set of geometries representative of the general case. The β values used have been 2.4 and 2.5.

However, e.g. Booth et al. [2] conclude that asymptotic scaling for SU(2) gauge theory begins at $\beta > 2.85$, so there is reason to suspect that the simulation results could contain significant lattice artefacts. Previous estimates show that finite size effects of our simulations are unimportant, while the conclusion that scaling (as opposed to asymptotic scaling) has been achieved at $\beta = 2.4$ is somewhat more questionable for larger configurations and excited states [3]. It is therefore expected that a continuum extrapolation could possibly yield different energies and point out artefacts in a parameterization of the energies while making the physical content clearer. Such an extrapolation is the object of this work.

The geometries to be simulated here were chosen to be squares and tilted rectangles [(R) with $x = y$ and (TR) in figure 1], because the simple model described below works for them and these geometries also exhibit the largest binding energies. The β values (and lattice sizes) used were $\beta = 2.35, 2.4$ ($16^3 \times 32$), 2.45 ($20^3 \times 32$), 2.5 ($24^3 \times 32$) and 2.55 ($26^3 \times 32$).

2 A model for four-quark energies

A model for the energy of four static quarks with explicit gluonic degrees of freedom removed has been developed by Green and coworkers [1, references therein]. In this model a potential matrix is diagonalized with different two-body pairings as basis states. The basis states for some simulated configurations are shown in

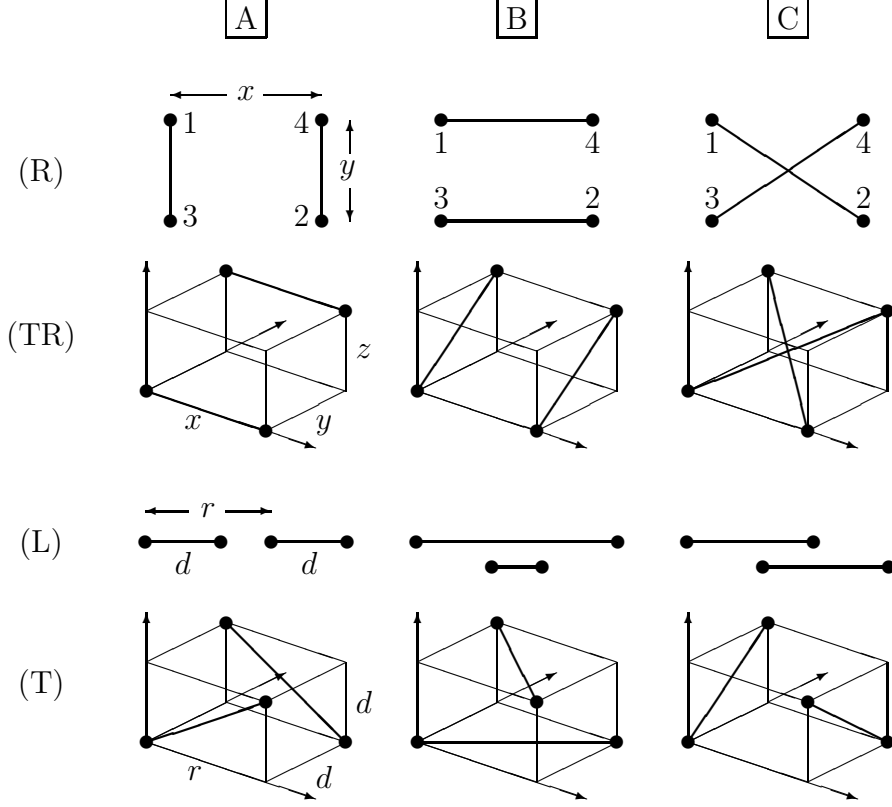


Figure 1: Some of the simulated four-quark geometries and their two-body pairings.

figure 1. For example, in the case of two basis states A and B, the eigenvalues λ_i are obtained from

$$[\mathbf{V} - \lambda_i \mathbf{N}] \Psi_i = 0, \quad (1)$$

with

$$\mathbf{N} = \begin{pmatrix} 1 & f/N_c \\ f/N_c & 1 \end{pmatrix} \quad \text{and} \quad \mathbf{V} = \begin{pmatrix} v_{13} + v_{24} & \frac{f}{N_c} V_{AB} \\ \frac{f}{N_c} V_{BA} & v_{14} + v_{23} \end{pmatrix}, \quad (2)$$

where v_{ij} represents the static two-body potential between quarks i and j . V_{AB} comes from the perturbative expression

$$V_{ij} = -\mathcal{N}(N_c) \mathbf{T}_i \cdot \mathbf{T}_j v_{ij}, \quad (3)$$

where for a colour singlet state $[ij]^0$ the normalization is chosen to give $\langle [ij]^0 | V_{ij} | [ij]^0 \rangle = v_{ij}$. The four-quark binding energies E_i are obtained by

subtracting the internal energy of the basis state with the lowest energy, e.g.

$$E_i = \lambda_i - (v_{13} + v_{24}).$$

A central element in the model is a phenomenological factor f appearing in the overlap of the basis states $\langle A|B \rangle = f/N_c$ for $SU(N_c)$. This factor is a function of the spatial coordinates of all four quarks, making the off-diagonal elements of \mathbf{V} in eq. 2 *four-body* potentials, and attempts to take into account the decrease of overlap from the weak coupling limit, where $\langle A|B \rangle = 1/N_c$. Perturbation theory to $O(\alpha^2)$ also produces the two-state model of eq. 1 with $f = 1$ [4]. Several parameterizations for f have been suggested, a general form being

$$f = f_c e^{-k_A b_S A - k_P \sqrt{b_S} P}. \quad (4)$$

Here b_S is the string tension, f_c a normalization constant and k_A, k_P multiply the minimal area and perimeter bounded by the four quarks respectively. In this work either the normalization or the perimeter term is omitted from eq. 4.

This simple version of the “ f -model” works for quarks in the corners of squares and (tilted) rectangles [(R) and (TR) in fig. 1], but fails to predict some features of non-planar geometries, e.g. the doubly degenerate ground state energy of a regular tetrahedron [(T) with $r = d$]. In section 5 there will be introduced a generalization of the model that is capable of reproducing this degeneracy.

3 Extrapolating to the Continuum

3.1 Setting the scale

Previously the scale in our simulations has been set by equating to the experimental continuum value the string tension $b_S = \lim_{r \rightarrow \infty} F(r)$, where $F(r)$ is the force between two static quarks, in lattice units. The string tension, however, was obtained by fitting the lattice parameterization of two-body potential to values from simulations at $r/a = 2, \dots, 6$ and not as $r \rightarrow \infty$.

Sommer [5] has designed a popular new way to set the scale that uses only intermediate distances. First the force $F(r/a)$ between two static quarks at separation r/a is calculated. By solving

$$(r_0/a)^2 F(r_0/a) = c \quad (5)$$

with $c = 1.65$ for r_0/a , we get the equivalent of the continuum value $r_0 \approx 0.5$ fm in lattice units. The constant on the right-hand side of eq. 5 has been chosen to correspond to a distance scale where we have best information on the force between static quarks. According to the widely cited paper of Buchmüller and

Tye [6] various nonrelativistic effective potentials which successfully model heavy quarkonia agree in the radial region 0.1 to 1.0 fm and predict r.m.s. radii from 0.2 to 1.5 fm for $\bar{c}c$ and $\bar{b}b$ systems. Even though these effective potentials are not the same as the QCD potential between static quarks, the distance scale where we have the best experimental evidence seems to be around 0.5 fm. A different estimate is given by Leeb et al. [7], who fit modified Cornell and Martin potentials to meson masses and claim that the known mesons determine the potential model-independently only between $r = 0.7$ fm and $r = 1.8$ fm.

In the Cornell [8] and Richardson [9] potential models the constant 1.65 in eq. 5 corresponds to $r_0 = 0.49$ fm. On the other hand, the Martin model [10], with the strange quark counted as heavy, gives $r_0 = 0.44$ fm and the modified Cornell and Martin potentials of ref. [7] result in 0.56 fm and 0.44 fm respectively (the published parameter values are incorrect ¹).

Choosing $c = 2.44$ as the scale setting constant makes the Richardson, modified Cornell and modified Martin potentials agree on $r_0 = 0.66$ fm with the basic Cornell and Martin models giving $r_0 = 0.64$ fm and 0.625 fm respectively. These models are clearly in better agreement at $c = 2.44$ than at $c = 1.65$. However, it is not excluded that the agreement may be accidental due to uncertainties in the models.

To set the scale, a lattice parameterization of the two-quark potential was first fitted to values obtained from simulations at $r/a = 2, \dots, 6$ for each β . The parameterization used was

$$v_L(r) = -\left(\frac{e}{r}\right)_L + b_S r + v_0, \quad (6)$$

where the on-axis lattice Coulomb potential is [11]

$$\begin{aligned} \left(\frac{1}{r}\right)_L &= \pi a^3 \int_{-\pi/a}^{\pi/a} \frac{dk_1 dk_2 dk_3}{(2\pi)^3} \frac{e^{-irk_1}}{\sum_{i=1}^3 \sin^2(k_i a/2)} \\ &\approx \frac{\pi}{L'^3} \sum_{\vec{q}} \frac{\cos(rq_1)}{\sum_{i=1}^3 \sin^2(q_i a/2)} \end{aligned} \quad (7)$$

$$aq_i = -\pi, \frac{\pi}{L'}, \dots, \frac{\pi(2L' - 1)}{L'}. \quad (8)$$

Here L' is twice the number of spatial sites along one axis. The fit results are presented in table 1 for data from tilted rectangle and square geometry runs performed in Helsinki, and $\beta = 2.5$ square runs from Wuppertal.

The force was calculated from this parameterization by the finite difference

$$F(r_I) = \frac{V(r) - V(r - d)}{d}, \quad (9)$$

¹Personal communication with H. Leeb.

β	e	$b_S a^2$	$v_0 a$	χ^2
2.35	0.255(12)	0.0985(15)	0.557(9)	2.6
2.35(TR)	0.260(5)	0.0978(7)	0.562(4)	1.0
2.4	0.248(7)	0.0709(10)	0.554(6)	0.1
2.4(TR)	0.238(9)	0.0716(13)	0.546(7)	0.18
2.45	0.244(5)	0.0494(7)	0.551(4)	0.04
2.45(TR)	0.238(5)	0.0507(6)	0.545(4)	0.05
2.5	0.226(5)	0.0373(7)	0.531(4)	0.55
2.5(TR)	0.233(4)	0.0367(5)	0.534(3)	0.53
2.5[W]	0.234(4)	0.0371(4)	0.536(3)	0.11
2.55	0.223(2)	0.0271(3)	0.522(2)	0.03
2.55(TR)	0.224(5)	0.0268(6)	0.523(4)	0.13

Table 1: Parameters of the lattice two-quark potential. [W] refers to data from Wuppertal, (TR) to tilted rectangles.

using $d = a$. Here

$$r_I = \sqrt{\frac{d}{[G(r-d) - G(r)]}}, \quad (10)$$

where

$$G(r) = \frac{1}{a} \left(\frac{1}{r} \right)_L \quad (11)$$

and r_I has been defined to remove $O[(a/r)^2]$ lattice artefacts from the argument of F , and to make $F(r_I)$ a tree-level improved observable [5].

After getting the force at points r_I/a , the expression $(r_I/a)^2 F(r_I/a)$ was interpolated to get r_0/a corresponding to eq. 5. Results for different β 's are presented in table 2, with lattice spacing a corresponding to $r_0 = 0.49$ fm and a^Π to $r_0^\Pi = 0.66$ fm. For comparison, a value of a^{bs} obtained from equating the string tension to the somewhat arbitrary continuum value $\sqrt{b_S} = 0.44$ GeV is presented. In all cases the a^Π consistently agrees with a^{bs} , whereas a disagrees, a^{bs}/a being ≈ 1.09 at each β . Choosing $\sqrt{b_S} = 0.478(4)$ GeV would move a^{bs} to the same value as a . A similar disagreement with the ratio of spacings being ≈ 1.04 was found by the SESAM collaboration working in SU(3) and using $c = 1.65$ in eq. 5 [12]. However, one should keep in mind that the quenched SU(2) string tension does not have to equal a phenomenological value.

As using $c = 2.44$ in the Sommer scheme produces better agreement with various continuum potential models and leads to agreement of a^Π and a^{bs} at continuum string tension value $b_S = 0.44$ GeV, it seems that $c = 1.65$ underestimates the lattice spacing. Using $c = 2.44$, corresponding to $r_0 \approx 0.66$ fm, is in our case

apparently a better choice than $c = 1.65$ and was chosen for this work, although the possibility that the difference is accidental cannot be excluded.

The $\beta = 2.5[W]$ values are calculated from potential data by a Wuppertal group doing simulations similar to ours [13]. The scales given by our and their data using the same analysis method agree well at $\beta = 2.5$, but the scales obtained from the published b_s values [0.0826(14) fm vs. 0.0864(5) fm] using the same data do not agree, which hints of the sensitivity of any intermediate distance determination of the string tension to the details of the fitting procedure. The errors in table 2 were estimated by adding or subtracting the one-sigma errors of the parameters of the lattice two-body potential, so systematic errors from e.g. the choice of r_0 are not included.

β	r_0/a	a [fm]	r_0^Π/a	a^Π [fm]	a^{bs} [fm]
2.35	3.76(2)	0.1302(6)	4.71(5)	0.1401(14)	0.1408(11)
2.35(TR)	3.77(2)	0.1299(7)	4.72(3)	0.1397(6)	0.1402(5)
2.4	4.45(5)	0.1101(10)	5.56(5)	0.1186(10)	0.1194(9)
2.4(TR)	4.44(2)	0.1103(5)	5.55(2)	0.1190(4)	0.1200(11)
2.45	5.34(4)	0.0918(7)	6.62(5)	0.0997(8)	0.0997(7)
2.45(TR)	5.27(5)	0.0929(7)	6.59(5)	0.1002(7)	0.1010(6)
2.5	6.18(5)	0.0793(5)	7.71(8)	0.0856(9)	0.0866(9)
2.5(TR)	6.21(5)	0.0789(5)	7.75(6)	0.0851(6)	0.0859(6)
2.5[W]	6.18(3)	0.0793(3)	7.71(5)	0.0856(6)	0.0864(5)
2.55	7.26(5)	0.0675(5)	9.04(6)	0.0730(5)	0.0741(7)
2.55(TR)	7.29(10)	0.0673(9)	9.08(12)	0.0727(10)	0.0734(8)

Table 2: Values of r_0/a and a for each β . r_0^Π/a and a^Π are calculated using $c = 2.44$ in eq.5.

The values of r_0 obtained agree with the relation $r_0 = \sqrt{(c - e)/b_s}$ using c from eq. 5 and e, b_s from the fit of the two-body parameterization of eq. 6.

A criterion for scaling of the two-body potential is equality of the parameter e for fits in the same physical distance range. In our case the fit range is shorter at higher β 's, and the values in table 1 support scaling at $\beta = 2.5$ and $\beta = 2.55$.

We can fit the relation between a and g ,

$$a = \frac{1}{\Lambda_{LAT}} e^{-\frac{\beta}{4N_c\beta_0}} \left(\frac{2N_c\beta_0}{\beta} \right)^{-\frac{\beta_1}{2\beta_0^2}} \left\{ 1 + A_1/\beta + A_2/\beta^2 + O(1/\beta^3) \right\}, \quad (12)$$

to the values of a obtained. Here, as usual, $\beta_0 = \frac{11}{3} \frac{N_c}{16\pi^2}$ and $\beta_1 = \frac{34}{3} \left(\frac{N_c}{16\pi^2} \right)^2$. Using Michael's result from ref. [14], let us fix $\sqrt{b_s}/\Lambda_{LAT} = 31.9$. Fitting to all

the values of a^{II} results in $A_1 = -4.24(32)$, $A_2 = 15.0(8)$ with $\chi^2 = 0.4$. The χ^2 value is per d.o.f. as elsewhere in this paper.

Using results of the former fit to get the β -function $b \equiv \partial\beta/\partial\ln a$ used results in $b = -0.304(5)$ at $\beta = 2.4$. This is in better agreement with the recent non-perturbative estimates $b = -0.302$ in ref. [15] and $b = -0.35(2)$ in ref. [16] than the value $b = -0.277(4)$ obtained by matching potentials at two β values [17].

3.2 Extrapolating two-body potentials

To extrapolate to the continuum, we need values of energies at different β 's but corresponding to the same physical size. Two-body potentials were interpolated from the values given by the lattice parameterization. Figure 2 shows an extrapolation of some of the two-body potentials involved in tilted rectangles. Others (from a total of 29) look similar – more pictures can be seen in ref. [18].

Linear (quadratic) fits with all data points included give χ^2 values from 15 to 35 (1.8 to 3.5), while cutting the $\beta = 2.35$ point off improves these to from 8 to 17 (0.5 to 1.5). Continuum energies given by the latter quadratic extrapolations are 6-8% higher than by the quadratic extrapolations including the $\beta = 2.35$ data.

The 29 quadratically extrapolated continuum potentials can be parameterized using eq. 6 with the lattice coulomb term replaced by e/r and $e = 0.21(11)$, $b_S = 5.11(80) \text{ fm}^{-2}$ and $v_0 = 9.38(11) \text{ fm}^{-1}$ ($\chi^2 = 0.4$). The value of the string tension corresponds to $\sqrt{b_S} = 0.446(37) \text{ GeV}$, which agrees well with the continuum value used to obtain the a^{b_S} in table 2.

The lattice artefact at each β , i.e. difference from quadratically extrapolated continuum energy, has a linear dependence on the inverse separation of the quarks in lattice units squared $(a/R)^2$. The slopes of this dependence at each β are within errors of each other, the average being 0.9(2).

3.3 Extrapolating the binding energies

The continuum extrapolations were performed for the square and tilted rectangle geometries, as the simple f -model works for them and allows the interpolation of binding energies to distances which are non-integer multiples of the lattice spacing. The ground state energy is given by

$$E_0 = \frac{\{2v_{s1} - 2v_{s2} + f^2(v_{s2} - v_d)\} + \sqrt{[2v_{s2} - 2v_{s1} - f^2(v_{s2} - v_d)]^2 - f^2(-4 + f^2)(v_d - v_{s2})^2}}{-2 + 0.5f^2}, \quad (13)$$

where v_{s1}, v_{s2}, v_d denote the two-body potentials along the shorter and longer side and the diagonal of the rectangle, respectively.

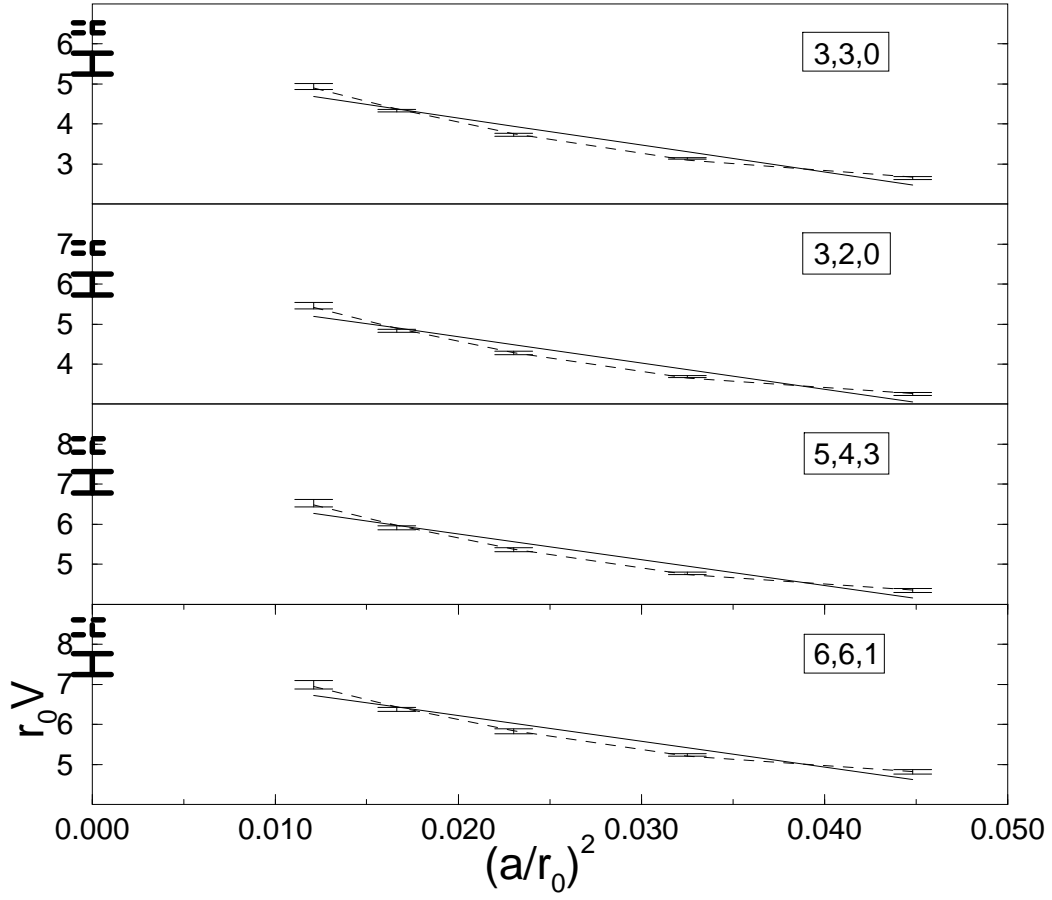


Figure 2: $r_0 V$ vs. $(a/r_0)^2$ for some two-body potentials, dimensions x, y, z shown in lattice units at $\beta = 2.5$

The two-parameter model of eq. 4 (with f_c , k_A or k_A , k_P) was fitted to the energies of squares and tilted rectangles separately. Result of extrapolating from these values is presented in figure 3 for tilted rectangles. Similar interpolations and extrapolations were performed for squares with sizes $2a, \dots, 6a$ at $\beta = 2.5$. Slopes for 11 of the 13 extrapolated energies were consistent with zero, supporting scaling of the binding energies at $\beta \geq 2.35$. Linear fits have low χ^2 values and are more reliable than quadratic fits, which introduce an unnecessary extra parameter and lead to very large errors on the continuum values.

4 The f -model in the continuum

4.1 Extrapolation of the parameters of f

The parameters of the factor f were extrapolated from values given by a fit to the combined energies of squares and tilted rectangles, as shown in table 3 for parameterizations with either the normalization or perimeter term omitted from eq. 4.

β	f_c	k_A	χ^2	k_A	k_P	χ^2
2.55	0.974(17)	0.77(6)	0.9	0.71(10)	0.020(16)	1.0
2.5	0.992(17)	0.76(4)	0.3	0.73(8)	0.008(13)	0.3
2.45	0.925(10)	0.64(3)	1.0	0.49(4)	0.057(8)	1.2
2.4	0.864(15)	0.57(2)	1.25	0.38(4)	0.087(10)	1.25
2.35	0.843(8)	0.57(2)	1.4	0.36(3)	0.101(5)	1.1

Table 3: Two-parameter f -models fitted to the square and tilted rectangle data.

Typical values of f are quite constant at different β 's, as shown in fig. 4, having slopes from $-3.0(4)$ to $2.5(3)$. These slopes are a reflection of the behaviour of the two-body potentials used to calculate the f 's. The parameters f_c , k_A and k_P are extrapolated in figure 5.

The lattice artefacts of masses are known to behave roughly as a^2 , but no theoretical justification exists for such behaviour of the artefacts of f . Therefore extrapolation results assuming this dependence should be given less weight than fits of the model to continuum extrapolated energies presented below. These two approaches agree for values of f in the continuum, while for the parameters of f the quadratic extrapolations roughly agree with values obtained from continuum fits of the model as can be seen in table 6.

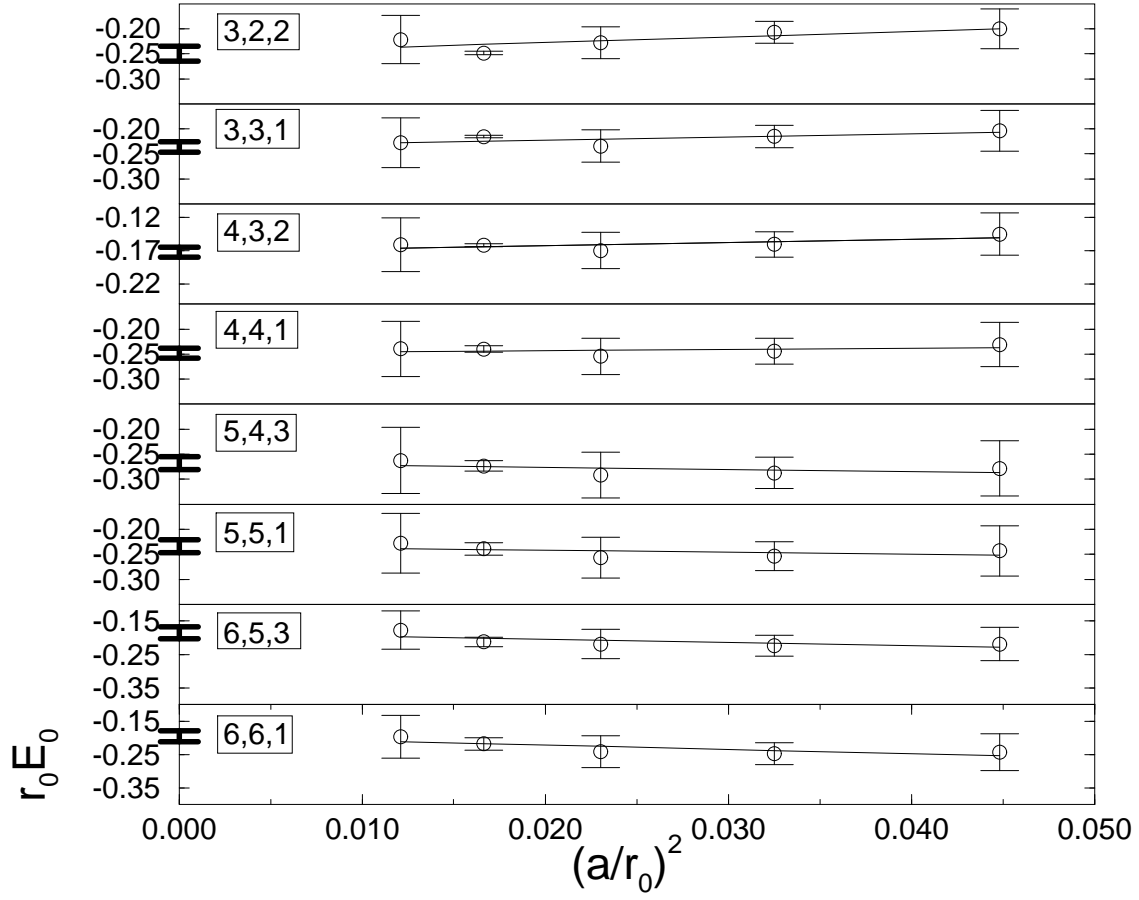


Figure 3: $r_0 E_0$ vs. $(a/r_0)^2$ for tilted rectangles with dimensions in lattice units shown at $\beta = 2.5$

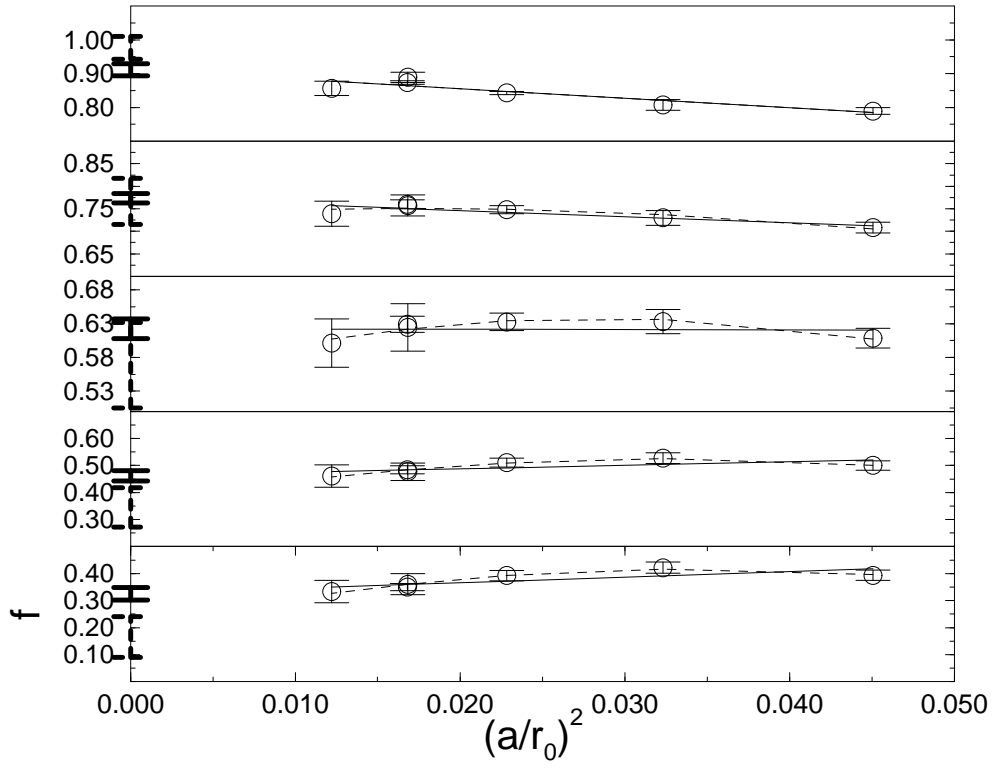


Figure 4: A continuum extrapolation of f 's for squares with length of a side from $2a$ (top) to $6a$ (bottom) at $\beta = 2.5$.

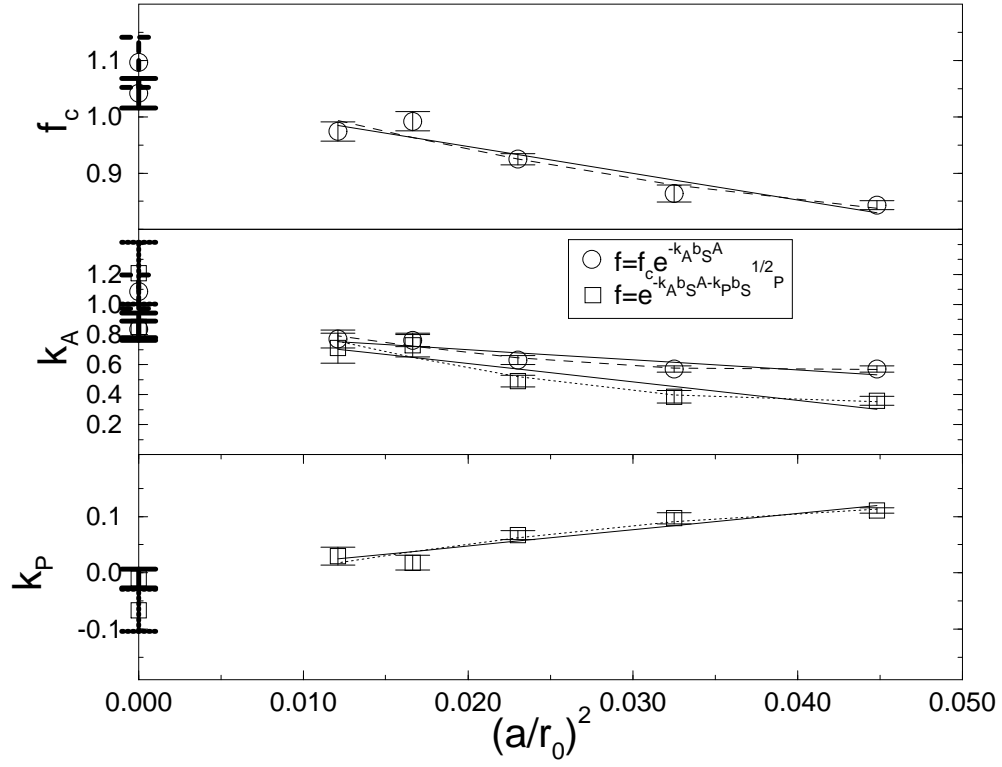


Figure 5: f_c , k_A and k_P continuum extrapolations.

4.2 Continuum fit

The fit data for all linear extrapolations is presented in table 4 and for all quadratic extrapolations in table 5.

Fit and parameter extrapolation results can be seen in table 6. Fits were also performed with quadratic extrapolations for two-body potentials and linear for four-bodies and are denoted “linear/quadratic” in the table. The parameter extrapolations have two χ^2 values, one for each of the extrapolated parameters.

$x/a, y/a, z/a$	$f(E_0)$	$E_0[\text{fm}^{-1}]$	$v_{s1}[\text{fm}^{-1}]$	$v_{s2}[\text{fm}^{-1}]$	$v_d[\text{fm}^{-1}]$
2,2,0	0.92(6)	-0.515(25)	7.44(34)		8.26(30)
3,2,2	0.88(6)	-0.379(15)	8.34(39)	8.432(40)	9.14(40)
3,3,0	0.77(2)	-0.439(10)	8.38(39)		9.17(39)
3,3,1	0.84(4)	-0.358(11)	8.43(40)	8.55(40)	9.28(40)
4,3,2	0.69(3)	-0.261(12)	8.84(40)	9.07(40)	9.84(40)
4,4,0	0.62(2)	-0.430(9)	8.98(31)		9.89(31)
4,4,1	0.65(2)	-0.376(15)	9.08(40)	9.15(40)	10.02(40)
5,4,3	0.48(2)	-0.406(19)	9.63(40)	9.63(40)	10.68(40)
5,5,0	0.46(2)	-0.388(14)	9.55(30)		10.59(31)
5,5,1	0.48(2)	-0.354(20)	9.63(40)	9.69(40)	10.71(40)
6,5,3	0.35(2)	-0.281(27)	10.07(40)	10.15(40)	11.30(40)
6,6,0	0.33(2)	-0.334(19)	10.06(31)		11.25(32)
6,6,1	0.32(2)	-0.296(25)	10.15(40)	10.19(40)	11.38(40)

Table 4: Continuum fit data with linear extrapolations

All fits and extrapolations predict f_c to be one or very slightly above. If it is set to one the fit to linear data and linear extrapolation give a k_A somewhat below one, while the linear/quadratic fit has k_A approximately one and the fit to quadratic data has a value slightly above unity. Since the linear/quadratic fits have low χ^2 values and are most reliable for two-body potentials and four-quark binding energies, our best estimates for the continuum values are $f_c = 1$, $k_A = 1.0(1)$ and $k_P = 0$. The perimeter term should become unimportant in the continuum limit [19], which is indeed observed. Thus the only parameter with physical significance is k_A .

Continuum fits were also performed for squares extrapolated using the original value $c = 1.65$ in Sommer’s equation 5. The resulting values of f_c and k_A for all linear and quadratic fits were within errors with fits to extrapolations using $c = 2.44$. As another test linear/quadratic and quadratic fits were performed with two-body potentials extrapolated with the $\beta = 2.35$ point cut off, with similar results but higher χ^2 values.

$x/a, y/a, z/a$	$f(E_0)$	$E_0[\text{fm}^{-1}]$	$v_{s1}[\text{fm}^{-1}]$	$v_{s2}[\text{fm}^{-1}]$	$v_d[\text{fm}^{-1}]$
2,2,0	0.90(16)	-0.40(11)	9.29(17)		9.95(18)
3,2,2	0.86(8)	-0.46(13)	9.70(18)	9.73(18)	10.52(20)
3,3,0	0.75(11)	-0.43(10)	10.09(19)		10.88(21)
3,3,1	0.68(5)	-0.29(14)	9.73(18)	9.89(19)	10.65(20)
4,3,2	0.55(6)	-0.20(11)	10.22(19)	10.45(20)	11.22(22)
4,4,0	0.56(9)	-0.40(10)	10.68(20)		11.59(23)
4,4,1	0.52(5)	-0.30(15)	10.45(20)	10.53(20)	11.40(23)
5,4,3	0.37(4)	-0.33(19)	11.00(22)	11.00(22)	12.07(25)
5,5,0	0.35(7)	-0.32(11)	11.24(22)		12.31(26)
5,5,1	0.36(4)	-0.27(18)	11.00(22)	11.07(22)	12.10(25)
6,5,3	0.27(4)	-0.23(18)	11.46(23)	11.52(23)	12.69(28)
6,6,0	0.19(5)	-0.22(11)	11.76(24)		12.99(29)
6,6,1	0.21(4)	-0.20(29)	11.52(23)	11.56(23)	12.77(28)

Table 5: Continuum fit data with quadratic extrapolations

In the strong coupling limit a factor $\exp(-b_S A)$ appears in the diagonal elements of the Wilson loop matrix, A being the minimal surface bounded by straight lines connecting the quarks. The factor is closely related to f and originates from the sum of spatial plaquettes tiling the transition surface between two basis states. When moving to weaker couplings there exist correlated flux configurations for which the transition area is much smaller than A , which has been expected to lead to larger mixing among basis states [20]. If this is the case, it is not reflected in our best estimate of a k_A about one. A larger transition area could be explained by the finite width of actual flux tubes instead of simply lines as in strong coupling approximation.

5 How can the model be developed?

The failure of the simple f -model of eqs. 1 and 2 to predict the energies of the tetrahedral geometry has been proposed to be due to a dependence of the tetrahedral energy on the first excited state of the gluonic field in the static two-quark potential. This can be investigated using the fact that an increasing fuzzing level reduces the excited state overlaps $C_i, i \geq 1$ in the energy eigenstate expansion of the Wilson loop

$$\langle W(R, T) \rangle = \sum_n C_n(R) e^{-V_n(R)T}. \quad (14)$$

type	f_c	k_A	k_P	χ^2
all linear	1.08(3)	1.04(5)	0	0.8
all linear, $f_c = 1$	1	0.94(3)	0	1.3
linear extrapol.	1.04(3)	0.83(6)	0	2.6/3.3
linear extrapol. (II)	1	0.85(9)	-0.02(2)	2.3/2.6
linear/quadratic	1.04(4)	1.04(6)	0	0.7
linear/quadratic, $f_c = 1$	1	0.98(3)	0	0.8
all quadratic	1.08(8)	1.39(13)	0	0.4
all quadratic, $f_c = 1$	1	1.27(6)	0	0.5
quadratic extrapol.	1.10(5)	1.09(11)	0	2.7/0.4
quadratic extrapol. (II)	1	1.2(2)	-0.08(4)	0.8/1.6

Table 6: Continuum fit and parameter extrapolation results.

The overlaps $C_n(R) \geq 0$ have a normalization condition

$$\sum_n C_n(R) = 1.$$

Increasing the fuzzing level used in the calculation of four-body energies should worsen the convergence of any four-body energy dependent on the excited state(s). Our group has been using fuzzing level 20 with $c = 4$, while a group in Wuppertal doing related work has chosen 150 with $c = 2$ to maximize the ground state overlap. At $\beta = 2.5$ they obtain C_0 values from 0.81 to 0.98 on a 16^4 lattice.

We made runs at $\beta = 2.5$ on a $24^3 \times 32$ lattice with three different fuzzing levels used to calculate the four-quark energy of a regular tetrahedron. Ground state overlaps C_0 of two-quark paths at different separations $r/a, d/a$ and at different fuzzing levels are shown in table 7. The four-body operators are constructed from the same paths, and the relative quality of convergence of the binding energy E_4 as a series in T is also shown.

The table shows that best convergences of the four-quark energies are obtained when the two-body paths have practically no overlap with gluonic excitations. Therefore the only way excitations can contribute is through overlaps of two-quark paths with excited states of gluon fields between other quark pairs. This contribution is likely to be significant; e.g. Isgur-Paton string model [21] with $N=1$ and $N=2$ predicts overlap between 1s and 2s states to be ≈ 0.4 when the centres of two parallel fluxtubes are separated by ≈ 0.7 fm. This can be seen from fig. 6.

The simple f -model of eqs. 1 and 2 can now be extended by using (in addition to the A, B, C shown in figure 1) three additional basis states describing the same quark partitions but involving the first excited state of the two-body potential.

	FL=150	FL=20	FL=0
$r/a, d/a$	C_0 %	C_0 %	C_0 %
2,2	N/A interm.	100.0(1) best	98.2(1) worst
3,3	98.7(1) interm.	100.0(1) best	96.7(1) worst
4,4	98.2(2) “best”	99.7(1) “best”	94.3(1) worst
5,5	97.9(2) interm.	99.5(1) best	91.1(1) worst
6,6	98.0(2) interm.	99.1(1) best	85.3(1) worst
7,7	99.1(4) interm.	98.0(1) best	N/A worst

Table 7: Ground state overlaps and E_4 convergence at different fuzzing levels (FL) and interquark distances.

The resulting 6×6 matrices contain two new gluon field overlap factors f^a and f^c similar to f , which however measure the overlap between an excited and ground state basis state and two excited basis states respectively. Solving the determinant analogous to eq. 1 gives for a regular tetrahedron two degenerate and two non-degenerate energy eigenvalues. The degenerate negative ground state energy of a regular tetrahedron would correspond to the lower of the degenerate eigenvalues, while it is harder for the model to predict the third eigenenergy from simulations since it is dominated by gluonic excitations as argued in ref. [1].

To estimate these eigenvalues, a parameterization for f from table 3 can be used with the minimal transition areas for regular tetrahedra calculated in ref. [22]. The energy of the first excited two-body state can be set to lie $a\pi/R$ higher than the ground state as has been observed in simulations. Because all the quarks in a regular tetrahedron have the same distance from each other, all the excited basis states have the same energy. Using these values, the simulation results for regular tetrahedra and a self consistency argument allows estimation of other parameters of the model.

The values obtained give the lower degenerate eigenvalue as the lowest eigenvalue when $f^c > 1$. This is now possible, since excited basis states with the lowest energies are normalized, *symmetric* combinations of one gluon field in the ground state and the other in an excited state. The overlap of two such basis states (f^c) therefore contains twice an overlap similar to f but with one excited gluon field in each of the basis states. In addition to this factor of two, f^c is likely to be larger

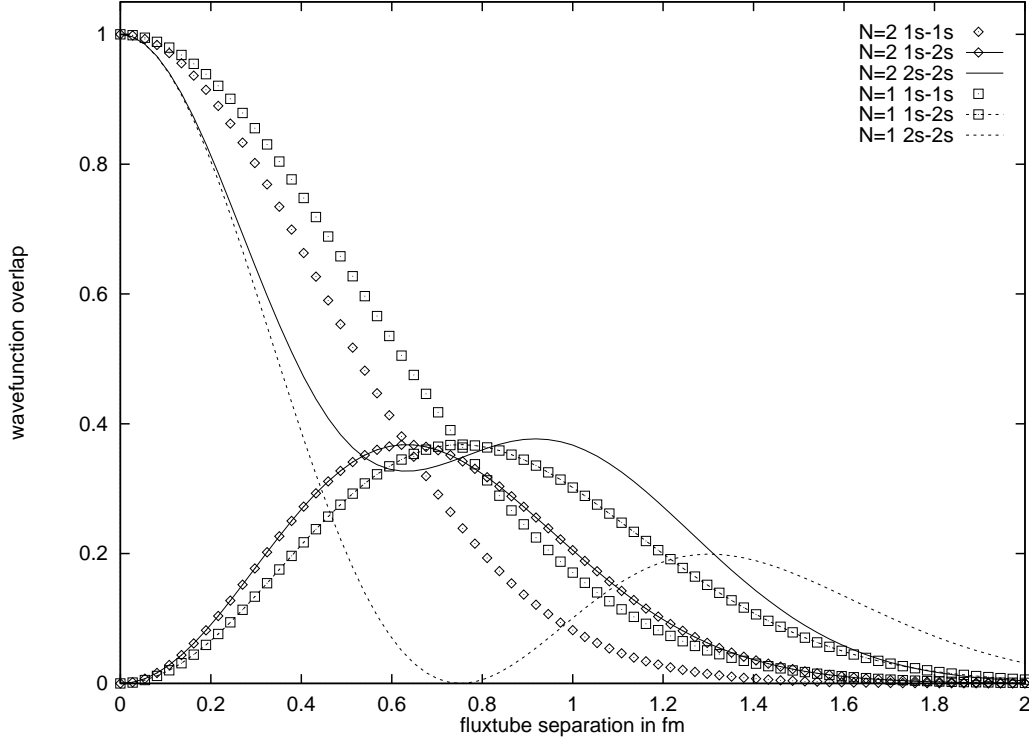


Figure 6: Overlaps of fluxtube wavefunctions as functions of fluxtube separation in the Isgur-Paton model with $N=1$ and $N=2$.

than f at large distances in a qualitatively similar way the Isgur-Paton 1s-1s and 2s-2s overlaps behave in figure 6. The values for the other new overlap factor f^a have a similar linear behaviour with the size of the system as is observed in figure 6 in the overlap of 1s-2s Isgur-Paton fluxtubes with separation in the same distance range, supporting reliability of the estimation scheme.

Work is in progress on applying this extended model to geometries more complicated than the regular tetrahedron [23].

6 Conclusions

The conclusions in this work can be summarized as follows:

1. Choosing $c = 2.44$ (corresponding to $r_0 \approx 0.66$ fm) in eq. 5 leads to better agreement of various continuum potential models with each other, and in our case gives lattice spacings that agree with those obtained from the string tension. This value of c thus seems a better choice than the original choice $c = 1.65$ ($r_0 \approx 0.49$ fm) by Sommer, although it cannot be excluded that

the difference is accidental due to uncertainties in the potential models and the quenched SU(2) string tension.

2. The lattice spacings a at the five values of β used in simulations give the β -function $b \equiv \frac{\partial\beta}{\partial\ln a} = 0.304(5)$ at $\beta = 2.4$, close to other recent estimates.
3. A quadratic extrapolation is preferred for two-body potentials, whose continuum parameterization is given in section 3.2. Four-quark binding energies are scaling from $\beta \geq 2.35$ and their values do not change significantly in the range of β values simulated. In practice the simulation results for the binding energies can thus be used directly, whereas it is recommended to use the continuum parameterization for two-body potentials to avoid introducing lattice artefacts into a four-quark energy model.
4. Parameter extrapolations and continuum fits of the simple f -model show that in the continuum, the normalization of the gluon field overlap factor f can be safely set to one and the perimeter term to zero, leaving the constant k_A multiplying the area as the only physically relevant parameter. Its value is about one and not $\ll 1$ as predicted for the transition area in ref. [20].
5. In our simulations, the effect on the four-quark energies of excited states of the gluon field between two quarks comes from the overlap of two-body paths with excited two-body fields of other quark pairings. An extended f -model using excited two-body potentials can reproduce the negative, degenerate ground state energy of a regular tetrahedron unlike the simple model based on ground state potentials. Estimates of parameters give the degenerate energy as the lowest eigenvalue when the excited state overlap factor $f^c > 1$. This is possible since f^c does not fall exponentially with increasing size of the system like f and has a factor of two built in when using excited basis states with the lowest energies.

Other possible extensions of the simple f -model include instanton effects (ref. [24]) and four-body interactions in the strong coupling limit (ref. [25]).

A study using microscopical flux distributions would be helpful in determining the relation of the shape of two- and four-quark fluxtubes and their overlaps to the parameterization of f . Our next project attempts this by using sum-rules similar to those derived by C. Michael [26].

7 Acknowledgement

I warmly thank A.M. Green for his support and encouragement. I would like to thank J. Lukkarinen and P. Laurikainen for discussions, C. Schlichter from

Wuppertal for kindly giving us their simulation results and S. Furui and B. Masud for communicating us their results of transition areas for tetrahedra. Funding from the Finnish Academy is gratefully acknowledged. Our simulations were performed on the Cray C94 at the Center for Scientific Computing in Espoo.

References

- [1] A. M. Green, J. Lukkarinen, P. Pennanen and C. Michael, Phys. Rev. **D 53**, 261 (1996).
- [2] S. P. Booth et al., Phys. Lett. **B 275**, 424 (1992).
- [3] A. M. Green, C. Michael, J. E. Paton and M. Sainio, Int. J. Mod. Phys. **E 2**, 479 (1993).
- [4] J. T. A. Lang, J. E. Paton and A. M. Green, Phys. Lett. **B 366**, 18 (1996).
- [5] R. Sommer, Nucl. Phys. **B 411**, 839 (1994).
- [6] W. Buchmüller and S.-H. H. Tye, Phys. Rev. **D 24**, 132 (1981).
- [7] H. Leeb, H. Fiedeldey, S. A. Sofianos, R. Lipperheide and M. F. de la Ripelle, Nucl. Phys. **A 508**, 365 (1990).
- [8] E. Eichten, K. Gottfried, T. Kinoshita, K. D. Lane and T. M. Yan, Phys. Rev. **D 21**, 203 (1980).
- [9] J. L. Richardson, Phys. Lett. **B 82**, 272 (1979).
- [10] A. Martin, Phys. Lett. **B 100**, 511 (1981).
- [11] C. B. Lang and C. Rebbi, Phys. Lett. **B 115**, 137 (1982).
- [12] U. Glässner et al., *First Evidence of N_f -Dependence in the QCD Interquark Potential*, Preprint HLRZ 96-20, appears on hep-lat/9604014 (1996).
- [13] G. S. Bali, K. Schilling and C. Schlichter, Phys. Rev. **D 51**, 5165 (1995).
- [14] C. Michael, Phys. Lett. **B 283**, 103 (1992).
- [15] J. Engels, F. Karsch and K. Redlich, Nucl. Phys. **B 435**, 295 (1995).
- [16] C. Michael, A. M. Green and P. S. Spencer, *Non-perturbative determination of beta-functions and excited string states from lattices*. To be published in Phys. Lett. **B**, appears on hep-lat/9606002.
- [17] S. Perantonis, A. Huntley and C. Michael, Nucl. Phys. **B 326**, 544 (1989).

- [18] P. Pennanen, *Four Quarks from Lattice to the Continuum*. To be published in Nucl. Phys. **B**, Lattice '96 Proceedings Supplements, appears on hep-lat/9608016.
- [19] S. Furui, A. M. Green and B. Masud, Nucl. Phys. **A 582**, 682 (1995).
- [20] H. Matsuoka and D. Sivers, Phys. Rev. **D 33**, 1441 (1987).
- [21] N. Isgur and J. Paton, Phys. Rev. **D 31**, 2910 (1985).
- [22] S. Furui and B. Masud, *An analysis of Four-quark Energies in $SU(2)$ Lattice Monte Carlo for the Tetrahedral geometry*, in preparation.
- [23] P. Pennanen and A. M. Green, in preparation.
- [24] T. Schafer and E. V. Shuryak, Phys. Rev. **D 54**, 1099 (1996).
- [25] D. Gromes, Zeit. Phys. **C 41**, 427 (1988).
- [26] C. Michael, Phys. Rev. **D 53**, 4102 (1996).